Asian Journal of Chemistry; Vol. 34, No. 7 (2022), 1735-1741

ASIAN JOURNAL OF CHEMISTRY

https://doi.org/10.14233/ajchem.2022.23750

Synthesis of Nickel Oxide Nanoparticles from *Syzygium cumini* Plant Fruit Pulp Extract: Study of their Antibacterial, Antifungal and Cytotoxic Activities on CHO Cells

LALITHA AMMADU KOLAHALAM[1], K.R.S. PRASAD[1,*], P. MURALI KRISHNA[2,*] and N. SUPRAJA[3]

[1]Department of Chemistry, Koneru Lakshmaiah Education Foundation, Green Fields, Vaddeswaram, Guntur 522502, India
[2]Department of Chemistry, Ramaiah Institute of Technology (Autonomous Institute, Affiliated to VTU), Bangalore-560054, India
[3]Nanotechnology Laboratory, Acharya N.G. Ranga Agricultural University, Tirupati-517502, India

*Corresponding authors: E-mail: krsprasad_fed@kluniversity.in; muralikp@msrit.edu

Received: 30 January 2022; *Accepted*: 5 March 2022; *Published online*: 15 June 2022; AJC-20848

The nickel oxide nanoparticles were synthesized using *Syzygium cumini* plant fruit pulp in a simple, ecofriendly and cost-effective procedure using the green chemistry route. The prepared nickel oxide nanoparticles were characterized by UV-visible (UV-Vis), Fourier transform infrared (FT-IR) spectroscopy, powder X-ray diffraction spectrometry (XRD), zeta potential (ZE), particle size (DLS), field emission scanning electron microscope (FE-SEM) analysis. The synthesized nanoparticles showed on an average of 16 to 31 nm in size. The synthesized nanoparticles were tested on several Gram-positive and Gram-negative bacteria and also on fungi, which showed less toxicity to them. Finally, the synthesized nanoparticles cytotoxic activity was tested on Chinese Hamster Ovary (CHO) cell lines, which showed cytotoxicity with IC_{50} value of 2.66 µg/mL.

Keywords: Nickel oxide nanoparticles, *Syzygium cumini,* Antibacterial activity, Antifungal activity, Cytotoxic activity.

INTRODUCTION

In recent decades, nanotechnology field is gaining much attention due to its enormous influence directly or indirectly on several fields such as food, agriculture, medicine, energy, electronics and space industries [1,2]. The nanomaterials showed unique properties due to the presence of very small size ranges from 1 to 100 nm at least in one dimension. Due to this small size, they exhibit high surface area/volume, surface charge, surface energy and porosity. The interaction with other molecules increases which directly influences their catalytic property [3,4]. Especially due to these properties the nanomaterials show their impact on science and technology fields, which leads to rising of the nanobiotechnology field [5,6]. In this context among the different metals and metal oxide nanoparticles, the NiO nanoparticles attracted several chemists due to their uses in the electrochemistry as battery electrodes, magnetic materials, catalysts, solid oxide fuel cells, gas sensors and in the absorption of inorganic pollutants and dyes [7].

On different microbial agents, NiO nanoparticles showed toxicity by producing ROS, leading to oxidative stress and finally releasing Ni^{2+} inside the cell [8] and so it also attracted the biologists due to its role as an antibacterial, antifungal, antioxidant and anticancer [9,10] agents. The NiO nanoparticles show good chemical stability, super conductivity nature and also magneto-optical, anti-inflammatory property and hence these nanoparticles can be applied in the field of biomedicine as well [11,12]. Generally, several physical and chemical routes for synthesizing the metals and metal oxide nanoparticles hydrothermal, sol-gel, co-precipitation, sonochemical, thermal decomposition, mechanical milling, laser ablation [2,13], *etc*. In these synthesis methods, several problems will be faced as they need costly solvents, and metal salts with expensive equipment and show negative effects on the surrounding environment and human lives. The NiO nanoparticles are synthesized *via* different physical and chemical routes also but through these synthesis routes several reducing and capping agents like sodium borohydrides, sodium hydroxide, hydrazine hydrate and urea are used and some of these are very expensive solvents. They may also limit their wide range of applications in this field [14].

In this concern, plants and microbes play a good route in the synthesis of nanoparticles. Through microbes' route undesired

effects on humans and the environment may cause and there will be the risk to the health and life of a human being also [15]. Therefore, a green route through plants showed a safe and cost-effective method for the synthesis of nanoparticles. Not only that alkaloids, terpenoids, glycosides, flavonoids, proteins, vitamins, polysaccharides and other organic substances that are present in the plants can enhance the antimicrobial and cytotoxic activity of nanoparticles and also works as a natural efficient fabricator for the synthesis of nanoparticles [16-21].

Herein, *Syzygium cumini* plant seed pulp was used for the synthesis of NiO nanoparticles. This plant is commonly called Malabar plum, jamun or black plum and belongs to Myrtaceae family [22,23]. The fruit of the plant contains anthocyanins, raffinose, glucose, fructose, citric acid, malic acid and gallic acid [24]. Multiple factors also influence the green synthesis of nanoparticles like concentration of plant extract, pH and synthesis procedure. *Syzygium cumini* plant was also used for the synthesis of iron, copper and silver [25-27] and zinc oxide [28] nanoparticles but no literature is available on the NiO nanoparticles synthesis from the fruit pulp. Currently preparation of NiO nanoparticles from the fruit pulp of *Syzygium cumini* plant and to study its antibacterial, antifungal activities and cytotoxicity effect of NiO nanoparticles on Chinese Hamster Ovary (CHO) cells.

EXPERIMENTAL

Nickel nitrate hexahydrate (98% AR), sodium hydroxide were purchased from Merck, India Pvt. Ltd. The Chinese Hamster ovary (CHO) cells were procured from National Centre for Cell Sciences (NCCS), Pune, India. The electronic spectrum of the material was measured in the range of 200-800 nm using Spectra 450 Shimadzu UV-visible spectrophotometer. Using dynamic light scattering (Nanopartica, Horiba, SZ-100) technique the size and distribution of nanoparticles were measured. The ATR (Attenuated Total Reflectance) Fourier-transform infrared (FT-IR) spectrum of the material was recorded between 4000-500 cm^{-1} with KBr pellet method. Using X-ray diffraction (XRD) analysis crystallinity of the nanoparticles was determined. Inspect F 50 field emission scanning microscope (FESEM) used to determine the shape and morphology of nanoparticles and energy dispersive X-ray (EDX) of the model (FEI-Quanta FEG 200F) was used to know the elemental analysis and chemical characterization of nanoparticles. The NETZSCH STA 449F5 instrument was used to carry out TG-DSC analysis of metal complex in nitrogen atmosphere (30-900 ºC) at a heating rate of 10 ºC min^{-1} using alumina powder as reference.

Extraction of the plant: Fresh fruits of the plant *Syzygium cumini* was collected from the campus of Koneru Lakshmaiah Education Foundation, Vaddeswaram, India. The collected fruits were washed with distilled water and dried in dark. Then the pulp of the fruit was grinded using mortar & pestle and collected the solid paste of the plant extract. The solid extract of about 20 g was dissolved in 100 mL distilled water and stirred at 60 ºC for about 2 h. The resultant solution was filtered and centrifuged to remove the other impurities and the final extract was stored at 4 ºC for further use.

Preparation of NiO nanoparticles from fruit pulp of *Syzygium cumini*: NiO nanoparticles were prepared by using sol-gel method. Nickel nitrate solution (50 mL, 0.1 M) was added to 50 mL aqueous plant extract solution slowly. The resultant mixture was stirred using magnetic stirrer and then heated with continuous stirring the solution at 80 ºC by adding 0.1 N NaOH to maintain pH 12 for about 2 h. The solution was transferred to China dish and continued the heating process on hot plate by increasing up to 150 ºC. After few hours, the aqueous layer in the solution was evaporated and a slurry gel was observed. Then the gel automatically ignited and burnt with glowing flames. After the completion of auto ignition process brown coloured ashes were formed. Collected the powder, grinded and calcinated at 600 ºC for 4 h. Blackish grey powder was collected and preserved for further analysis.

Biological studies

Antimicrobial activity: To analyze the effectiveness of the antimicrobial activity of biosynthesized NiO nanoparticles, three concentrations (170, 100, 50 ppm) of NiO nanoparticles were used on several Gram-positive (*Streptococcus aureus* and *Bacillus subtilis*), Gram-negative (*Sphingobacterium thalpophilum*, *Staphylococcus aureus*, *Pseudomonas aeruginosa*, *Escherichia coli*, *Sphingobacterium* sp, *Acinetobacter* sp., *Ochrobacterum* sp.) bacteria and also on fungi (*Aspergillus* sp., *Meyerozyma* sp, *Rhizobium oryzae*, *Trichoderma asperellum* and *Fusarium oxysporium*) by using disk diffusion agar analysis.

Cytotoxic activity of NiO nanoparticles: Using MTT [(3-(4,5-dimethylthiazol-2-yl)-2,5-diphenyltetrazolium bromide)] assay method the *in vitro* cytotoxic studies were observed on Chinese Hamster Ovary (CHO) cell lines. At 37 ºC in a humidified incubator these cells were grown under 5% CO_2/95% air in DMEM with 10% Fetal Bovine Serum (FBS) and in 96 well plates at the quantity of 0.2×10^6 cells per well plate the CHO cells were seeded. In a humidified incubator, the cells were treated with test compounds for 24 h and then with MTT of 20 µL of 50 mg/mL for 4 h followed by the addition of 200 µL of DMSO to the wells to dissolve the MTT formazan crystals. In a control experiment, without the presence of nanoparticles the cells were cultured in the same media. Immediately after the formation of the purple colour absorbance of the wells was analyzed at 570 nm. In these control cells, how much amount of formazan produced was considered to be 100% viability and the relative cell viability was calculated according to the quantity of MTT converted into insoluble formazan salt. Three independent experiments were done and ± SEM was calculated and reported as% of cell viability *vs.* concentration (µM). The IC_{50} value was calculated from the graph.

$$\text{Cell viability (\%)} = \frac{\text{Optical density of NiO NPs}}{\text{Optical density of control}} \times 100$$

Isolation of test organisms: Eight varieties of fungi (*Meyerozyma caribbica* and *guilliermondii*, *Aspergillus niger*, *flavus* and *oryza*, *Rhizopus oryzae*, *Trichoderma asperellum* and *Fusarium oxysporium*) varieties and ten varieties of bacterial species (*Staphylococcus aureus*, *Sphingobacterium thalpophilum*, *Escherichia coli*, *Pseudomonas aeruginosa*, *Sphingo-*

bacterium sp., *Acinetobacter* sp., *Ochrobactrum* sp., *Bacillus subtilis*, *Streptococcus aureus* and Uncultured bacterium) were isolated from the drinking water supply of the PVC pipeline in Tirupati, Chittoor district, India. Using potato dextrose agar, the fungal species were isolated and using nutrient agar medium the bacterial species were isolated through the serial dilution pour plate technique. Then they were maintained in potato dextrose agar slants for fungi and nutrient agar slants for bacteria for further analysis.

Statistical analysis: All the data reported were examined repeatedly for three trials and subjected to analysis using Statistical Package for the Social Sciences (SPSS) version 16.0. The data are reported as the mean ± SD and significant differences between mean values were determined with one way analysis of variance (CRD) followed by Duncan's multiple range test (DMRT) ($p < 0.05$).

RESULTS AND DISCUSSION

Formation of NiO nanoparticles from plant extract: Addition of nickel nitrate solution to the plant extract leads to the physico-chemical changes in the aqueous solution and also the natural products present in the plant extract *Syzygium cumini* change the nickel(II) ion to nickel oxide nanoparticles. The formation of NiO nanoparticles was completed in a short period of time with the change in colour from light green to dark colour.

UV visible studies: Synthesized NiO nanoparticles formation and stability were confirmed by the absorption peaks around 485 and 495 nm (Fig. 1). A small peak around 485 nm confirms the formation and stability of synthesized NiO nanoparticles. Peak around 495 nm occured due to the presence of alkaloids and other chemical constituents of the plant and so the peak was shifted to the higher wavelength side. It was also due to the presence of surface oxygen vacancies of NiO nanoparticles. Similar reports were also reported earlier [29,30].

Thermal studies: Thermal properties of NiO nanoparticles were characterized using thermogravimetric analysis (TGA) and differential scanning calorimetry (DSC). As shown in Fig. 2, 7.5% of mass of the sample loss in the temperature region (200-225 ºC) indicates the loss of the organic molecules present in nanoparticles. Further heating up to 900 ºC, the synthesized NiO nanoparticles showed 90% thermal stability may be due to NiO residue. In DSC curve, negligible two exothermic peaks between 200-400 ºC indicates the decomposition of the organic molecules.

Dynamic light scattering analysis: From Table-1, the synthesized NiO nanoparticles showed 16.5 nm size with 55.3 mV zeta potential. The nanoparticles stability is directly proportional to the magnitude of charge and more positive or negative charge value of zeta potential indicates the excellent physical colloidal stability [31]. Based on this, the synthesized NiO nanoparticles showed very good stability (Fig. 3a-b) and this may be due to the electrostatic repulsions between the respective particles.

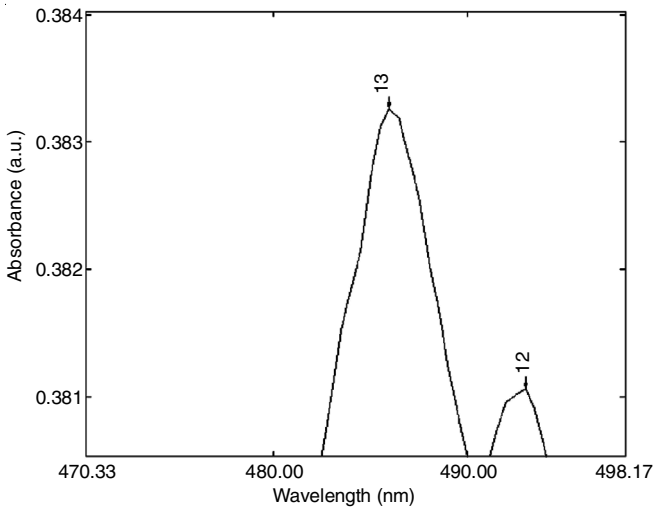

Fig. 1. UV-vis spectrum of synthesized NiO nanoparticles using *Syzygium cumini* plant extract

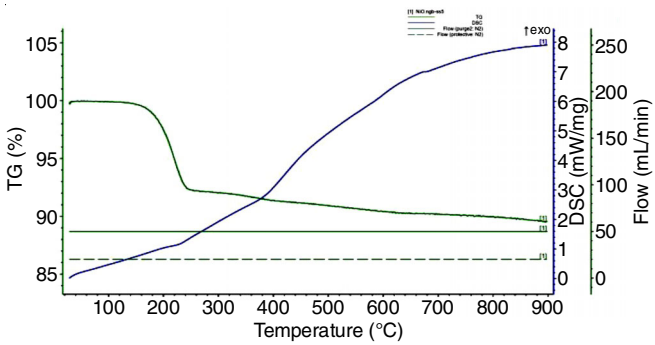

Fig. 2. TGA-DSC spectrum of synthesized NiO nanoparticles using *Syzygium cumini* plant extract

FT-IR studies: The FT-IR spectrum of synthesized NiO nanoparticles was recorded from 4000-500 cm^{-1}. In FT-IR spectrum of the sample showed peaks 3847-3617 cm^{-1} were observed which related to O-H and C-H bands of the plant extract. Further, peaks at 2966, 2359, 1918, 1741, 1695, 1524 and 1050 cm^{-1} observed related to the stretching vibrations of strong C-H (amines), -C≡C- of alkynes, C=O, C-N, N-H bending and -C-O-H in plane bands, respectively present in the plant extract (Fig. 4). The Ni-O vibration of the NiO nanoparticles was observed at 538 cm^{-1} band (Fig. 4).

TABLE-1
DYNAMIC LIGHT SCATTERING AND ZETA POTENTIAL DATA OF SYNTHESIZED NiO NANOPARTICLES

Particle size					Zeta potential		
Peak No.	S P area ratio	Mean (nm)	SD (nm)	Mode (nm)	Peak No.	Zeta potential (mV)	Electrophoretic mobility mean (cm^2/Vs)
1	1.00	16.5	1.0	16.3	1	-3.7	-0.000029
2	–	–	–	–	2	130.9	0.001016
3	–	–	–	–	3	33.2	0.000258
Total	1.00	16.5	1.0	16.3	Total	55.3	0.000429

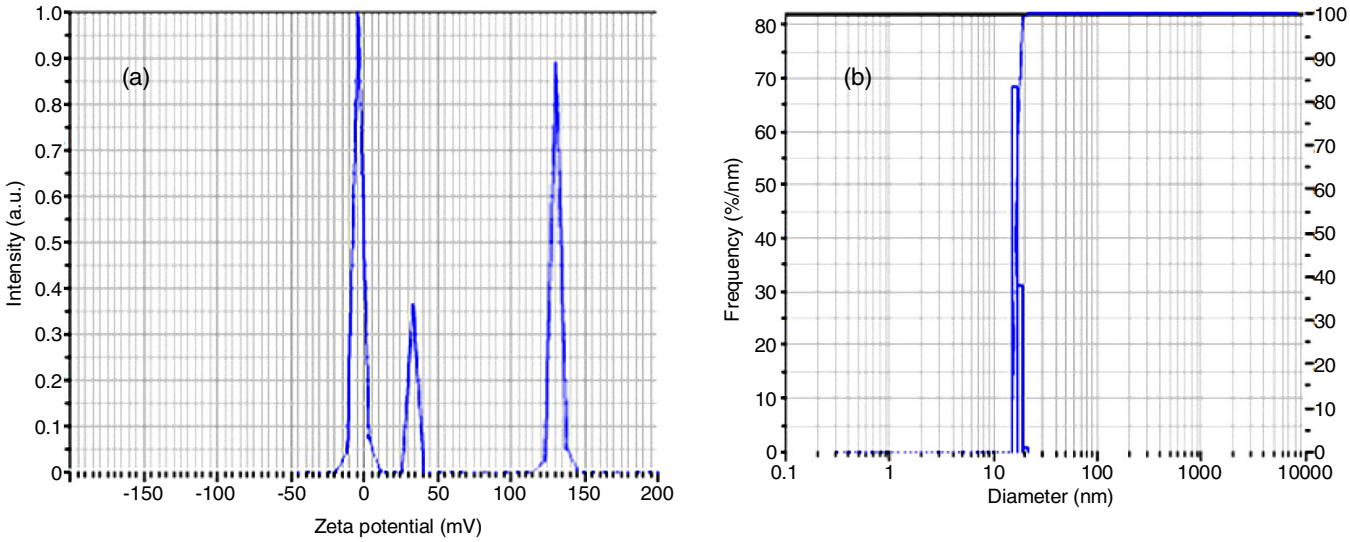

Fig. 3. DLS spectrum of synthesized NiO NPs from *Syzygium cumini* plant extract showing (a) zeta potential and (b) particle size

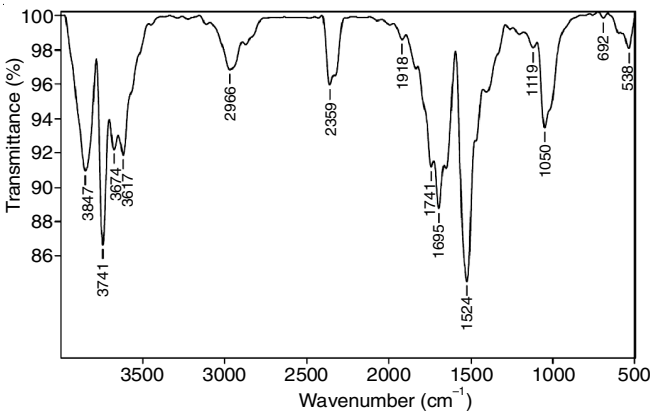

Fig. 4. FT-IR spectrum of synthesized NiO nanoparticles using *Syzygium cumini* plant extract

X-ray diffraction (XRD) analysis: Fig. 5 showed the XRD patterns of the synthesized NiO nanoparticles using *Syzygium cumini* plant extract. In XRD, the characteristic peaks

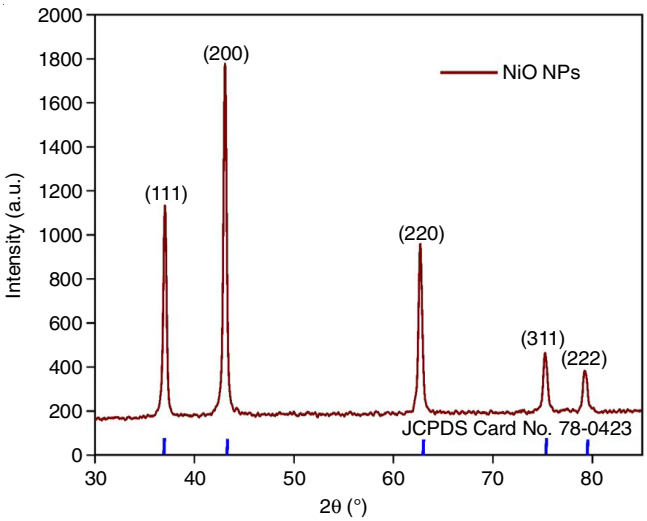

Fig. 5. XRD spectrum of synthesized NiO nanoparticles using *Syzygium cumini* plant extract

were found at 2θ (°) values of 36.99º, 43.14º, 62.69º, 75.30º and 79.26º. The obtained peaks were indexed as (111), (200), (220), (311) and (222). These XRD patterns were matched with JCPDS file no. 78-0423 and all the results were indexed to face-centered cubic (FCC) structure of NiO nanoparticles [29].

Morphology studies of nickel oxide nanoparticles: Using FESEM images, the structure of prepared NiO nanoparticles were found to be in rough cubic size with little agglomeration and the average size of nanoparticles were around 31.30 nm (Fig. 6). The results of JCPDS data of XRD and FESEM were almost correlated the size and shape of the nanoparticles. Energy dispersive X-ray (EDX) analysis is used for the elemental composition of NiO nanoparticles. Strong signals from the NiO atoms in the nanoparticles (Fig. 7) revealed that the NiO nanoparticles have Ni rich environment in the lattice.

Antimicrobial activity: From Tables 2 and 3, 170 ppm concentrated nanoparticles showed good antimicrobial activity when compared with other concentrations of 50 and 100 ppm. In them the Gram-negative bacteria of *E. coli* and *P. aeruginosa* species showed effective zone of inhibition in all the three concentrations. Regarding fungal species *M. guilliermondii* showed effective zone of inhibition in all the three concentrations when compared with remaining types. By the treatment of the metal ion causes structural changes, degradation and at last to cell death. This is due to the participation of the interacted nanoparticles in the building blocks of cell outer membrane and also in the process of inhibition there will be the loss of DNA replication ability. ATP producing enzymes and cellular proteins become inactivated followed by the ribosomal subunit protein expression inactivation and all these changes are due to the release of reactive oxygen species (ROS) [32]. After binding of nanoparticles to the cytoplasmic membrane, the electrostatic interaction between the positively charged nanoparticles and negatively charged cell membranes of microorganisms causes lysis of the bacterial and fungal cells. The antimicrobial activity is a dose-dependent one, which can be observed from the results that on decreasing the concentration of nanoparticles diameter of zone of inhibition also decreased.

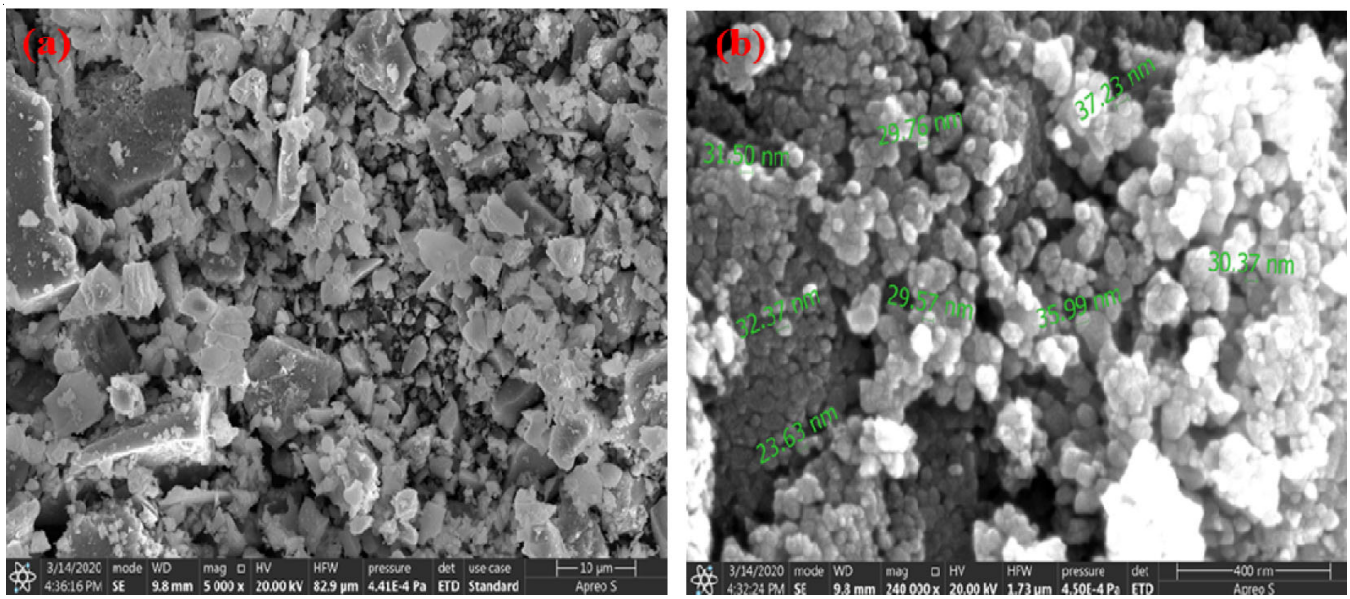

Fig. 6. FESEM images of synthesized NiO NPs using *Syzygium cumini* plant extract at different magnifications (a) at 10 µm and (b) at 400 nm

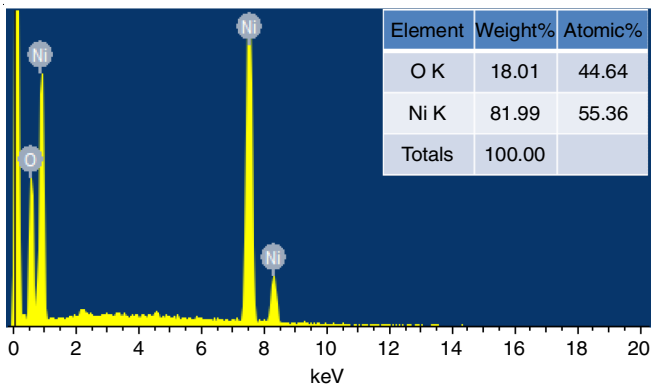

Fig. 7. EDX graph of synthesized NiO NPs using *Syzygium cumini* plant extract

TABLE-2
In vitro ANTIBACTERIAL STUDIES OF SYNTHESIZED NiO NANOPARTICLES

Bacteria	Zone of inhibition (mm)		
	170 ± 1.4 ppm	100 ± 1.1 ppm	50 ± 0.9 ppm
Gram-negative			
Sphingobacterium thalpophilum	1.3 ± 0.04^{bc}	1.4 ± 0.02^{d}	0.5 ± 0.05^{cd}
Staphylococcus aureus	2.5 ± 0.03^{a}	2.1 ± 0.05^{a}	1.6 ± 0.06^{a}
E. coli	2.5 ± 0.05^{a}	2.0 ± 0.04^{abc}	1.2 ± 0.07^{c}
Pseudomonas aeruginosa	2.4 ± 0.08^{bc}	2.2 ± 0.08^{ab}	2.0 ± 0.05^{cd}
Sphingobacterium sp	2.3 ± 0.06^{a}	1.9 ± 0.03^{a}	1.2 ± 0.16^{a}
Acinetobacter sp	2.6 ± 0.04^{b}	1.2 ± 0.04^{d}	1.0 ± 0.06^{b}
Ochrobactrum sp	2.2 ± 0.18^{de}	1.8 ± 0.01^{d}	0.8 ± 0.08^{d}
Gram-positive			
Bacillus subtilis	3.0 ± 0.14^{a}	2.3 ± 0.07^{d}	1.2 ± 0.04^{b}
Streptococcus aureus	2.5 ± 0.03^{a}	2.1 ± 0.05^{a}	1.6 ± 0.06^{a}
Uncultured bacterium	2.7 ± 0.17^{d}	2.0 ± 0.06^{abc}	0.3 ± 0.09^{d}
C.R.D. ($p \leq 0.05$)	0.232	0.202	0.155

The data presented is ± SE of three measurements; Data followed by the same letter are not significantly different at $p \leq 0.05$, whereas those followed by different letters are significantly different at $p \leq 0.05$; C.R.D. = Completely randomized design.

TABLE-3
In vitro ANTIFUNGAL STUDIES OF SYNTHESIZED NiO NANOPARTICLES

Fungi	Zone of inhibition (mm)		
	170 ± 1.4 ppm	100 ± 1.1 ppm	50 ± 0.9 ppm
Meyerozyma caribbica	2.3 ± 0.12^{b}	2.1 ± 0.08^{cd}	1.0 ± 0.02^{ab}
Aspergillus niger	1.5 ± 0.14^{c}	1.0 ± 0.22^{c}	0.4 ± 0.05^{a}
Meyerozyma guilliermondii	2.4 ± 0.05^{b}	2.0 ± 0.14^{d}	1.7 ± 0.07^{a}
Rhizopus oryzae	2.5 ± 0.08^{a}	2.0 ± 0.02^{ab}	0.7 ± 0.08^{c}
Aspergillus flavus	2.2 ± 0.06^{a}	1.5 ± 0.08^{ab}	1.0 ± 0.06^{a}
Aspergillus oryzae	1.9 ± 0.04^{c}	1.3 ± 0.06^{c}	0.2 ± 0.04^{a}
Trichoderma asperellum	1.9 ± 0.08^{a}	1.0 ± 0.05^{a}	0.4 ± 0.12^{b}
Fusarium oxysporium	2.0 ± 0.02^{a}	1.2 ± 0.04^{d}	0.6 ± 0.14^{c}
C.R.D. ($p < 0.05$)	0.220	0.190	0.160

The data presented is ± SE of three measurements; Data followed by the same letter are not significantly different at $p \leq 0.05$, whereas those followed by different letters are significantly different at $p \leq 0.05$; C.R.D. = Completely randomized design.

Cytotoxic activity of NiO nanoparticles: Using different concentrations of NiO nanoparticles *in vitro* cytotoxic effect of these nanoparticles were tested on Chinese Hamster ovary (CHO) cells. In a control experiment, cells were grown in the same media without the nanoparticles. Soon after the development of purple colour absorbance was recorded at 570 nm. Three independent experiments were carried out and mean ± SEM was calculated and the results were reported as (%) of cell viability *vs.* concentration (µM). To test the dosage effect of NiO nanoparticles different concentrations of 2,3,4,5,6 µg/mL of nanoparticles were taken and tested for cytotoxic studies. These results are shown in Figs. 8 and 9. On increasing the concentration of NiO nanoparticles decrease of cell viability percentage was observed. So, 6 µg/mL NiO nanoparticles concentration showed low percentage of cell viability and hence it showed good cytotoxic activity on Chinese Hamster Ovary (CHO) cells. The IC_{50} value of the CHO cell line is 2.66 µg/

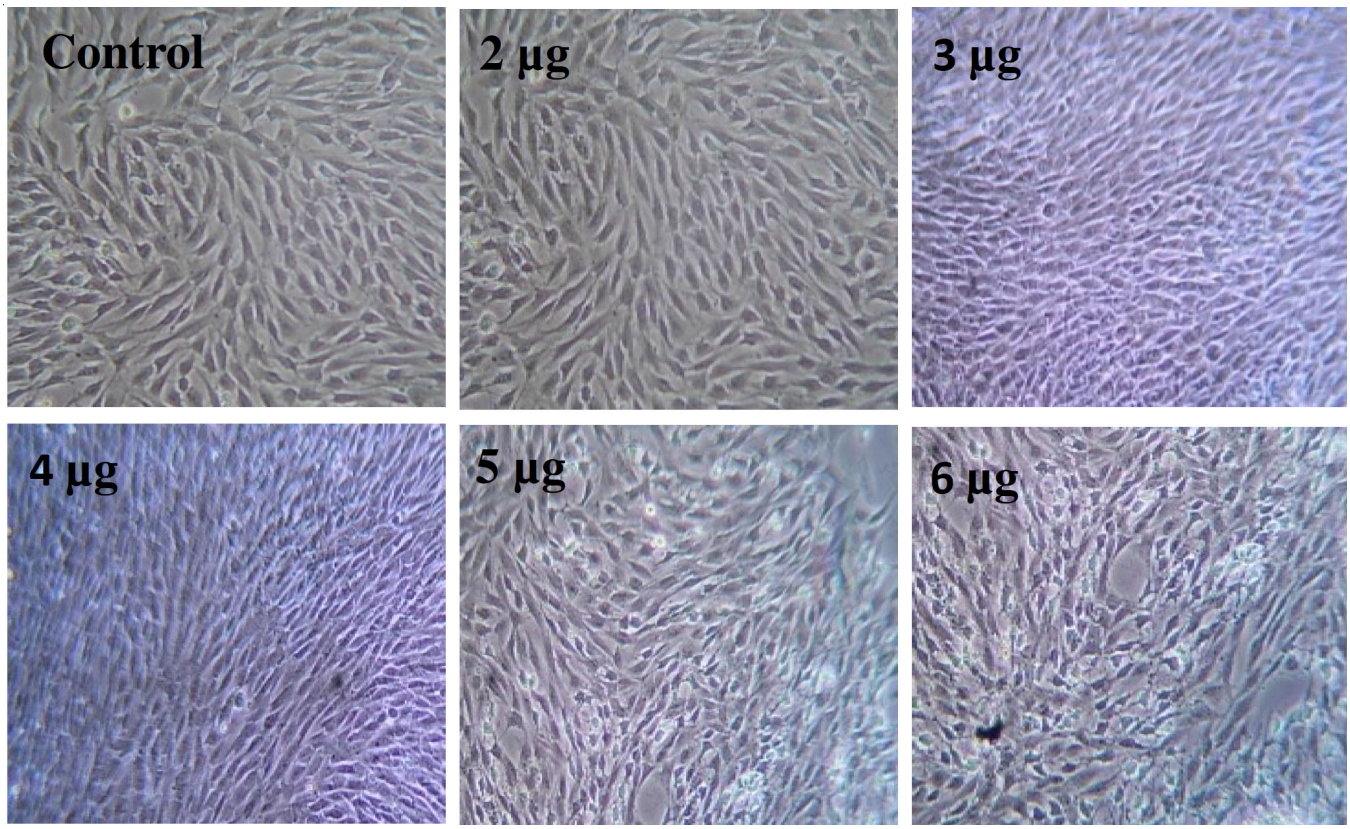

Fig. 8. Cytotoxic activity of synthesized NiO nanoparticles on CHO cancer cells from 2 to 6 µg/mL with control

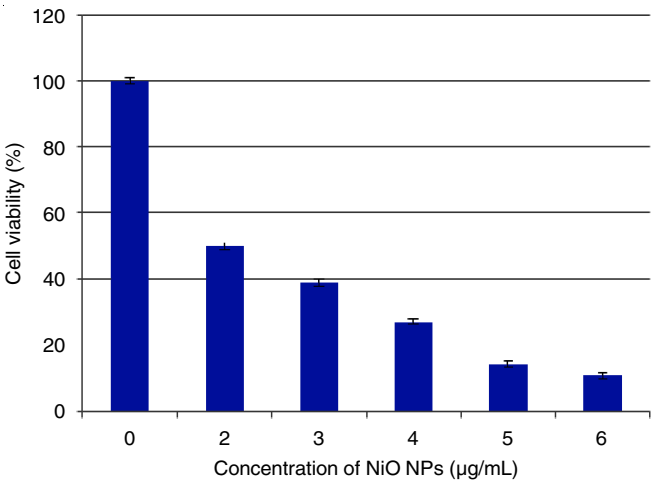

Fig. 9. Graphical representation of cytotoxic activity of synthesized NiO nanoparticles on CHO cancer cells from 2 to 6 µg/mL with control

mL. There is a need for deep study of size and shape dependent NiO nanoparticles in to mammalian cells and also its anti-microbial activity also.

Conclusion

In current work, the NiO nanoparticles were prepared from fruit pulp of *Syzygium cumini* plant with very fewer chemical reagents by sol-gel technique. The formation of NiO nanoparticles were confirmed by UV-visible, FT-IR, XRD, DLS and FESEM techniques. The prepared NiO nanoparticles act as a good antibacterial, antifungal and also a cytotoxic agent against Chinese hamster ovary (CHO) cell lines.

ACKNOWLEDGEMENTS

One of the authors (Lalitha A. K) is thankful to Koneru Lakshmaiah Education Foundation, Vaddeswaram, India, for providing necessary laboratory facilities and the financial support to carry out the (Ph.D.) work. The authors also thankful to Centre for Advanced Material Technology, Ramaiah Institute of Technology, Bangalore for thermal analysis.

CONFLICT OF INTEREST

The authors declare that there is no conflict of interests regarding the publication of this article.

REFERENCES

1. Y. Chen, Z. Fan, Z. Zhang, W. Niu, C. Li, N. Yang, B. Chen and H. Zhang, *Chem. Rev.*, **118**, 6409 (2018); https://doi.org/10.1021/acs.chemrev.7b00727
2. L.A. Kolahalam, I.V. Kasi Viswanath, B.S. Diwakar, B. Govindh, V. Reddy and Y.L.N. Murthy, *Mater. Today Proc.*, **18**, 2182 (2019); https://doi.org/10.1016/j.matpr.2019.07.371
3. B.N. Rashmi, S.F. Harlapur, B. Avinash, C.R. Ravikumar, M.R. Anil Kumar, H.P. Nagaswarupa, K. Gurushantha and M.S. Santosh, *Inorg. Chem. Commun.*, **111**, 107580 (2020); https://doi.org/10.1016/j.inoche.2019.107580
4. A. Munir, T. ul Haq, I. Hussain, A. Qurashi, U. Ullah, J. Iqbal and I. Hussain, *ChemSusChem*, **12**, 5117 (2019); https://doi.org/10.1002/cssc.201902505
5. J. Iqbal, B.A. Abbasi, R. Ahmad, T. Mahmood, B. Ali, A.T. Khalil, S. Kanwal, S.A. Shah, M.M. Alam, H. Badshah and A. Munir, *Appl. Microbiol. Biotechnol.*, **102**, 9449 (2018); https://doi.org/10.1007/s00253-018-9352-3

6. S. Andleeb, F. Tariq, A. Muneer, T. Nazir, B. Shahid, Z. Latif, S.A. Abbasi, I. Haq, Z. Majeed, S.U.-D. Khan, S.U.-D. Khan, T.M. Khan and D.A. Al Farraj, *Green Process. Synth.*, **9**, 538 (2020); https://doi.org/10.1515/gps-2020-0051
7. C.J. Pandian, R. Palanivel and S. Dhananasekaran, *Chin. J. Chem. Eng.*, **23**, 1307 (2015); https://doi.org/10.1016/j.cjche.2015.05.012
8. N. Gong, K. Shao, W. Feng, Z. Lin, C. Liang and Y. Sun, *Chemosphere*, **83**, 510 (2011); https://doi.org/10.1016/j.chemosphere.2010.12.059
9. A.A. Ezhilarasi, J.J. Vijaya, K. Kaviyarasu, M. Maaza, A. Ayeshamariam and L.J. Kennedy, *J. Photochem. Photobiol. B*, **164**, 352 (2016); https://doi.org/10.1016/j.jphotobiol.2016.10.003
10. B.A. Abbasi, J. Iqbal, T. Mahmood, R. Ahmad, S. Kanwal and S. Afridi, *Mater. Res. Express*, **6**, 0850a7 (2019); https://doi.org/10.1088/2053-1591/ab23e1
11. G.M. Whitesides, *Small*, **1**, 172 (2005); https://doi.org/10.1002/smll.200400130
12. B. Sasi, K.G. Gopchandran, P.K. Manoj, P. Koshy, P. Prabhakara Rao and V.K. Vaidyan, *Vacuum*, **68**, 149 (2002); https://doi.org/10.1016/S0042-207X(02)00299-3
13. S.A.M. Ealia and M.P. Saravanakumar, *IOP Conf. Ser. Mater. Sci. Eng.*, **263**, 032019 (2017); https://doi.org/10.1088/1757-899X/263/3/032019
14. F.T. Thema, E. Manikandan, A. Gurib-Fakim and M. Maaza, *J. Alloys Compd.*, **657**, 655 (2016); https://doi.org/10.1016/j.jallcom.2015.09.227
15. P. Anastas and N. Eghbali, *Chem. Soc. Rev.*, **39**, 301 (2010); https://doi.org/10.1039/B918763B
16. B.A. Abbasi, J. Iqbal, T. Mahmood, A. Qyyum and S. Kanwal, *Appl. Organomet. Chem.*, **33**, e4947 (2019); https://doi.org/10.1002/aoc.4947
17. B.A. Abbasi, J. Iqbal, R. Ahmad, L. Zia, S. Kanwal, T. Mahmood, C. Wang and J.-T. Chen, *Biomolecules*, **10**, 38 (2019); https://doi.org/10.3390/biom10010038
18. S. Hameed, A.T. Khalil, M. Ali, M. Numan, S. Khamlich, Z.K. Shinwari and M. Maaza, *Nanomedicine*, **14**, 655 (2019); https://doi.org/10.2217/nnm-2018-0279
19. L.P. Lingamdinne, Y.-Y. Chang, J.-K. Yang, J. Singh, E.-H. Choi, M. Shiratani, J.R. Koduru and P. Attri, *Chem. Eng. J.*, **307**, 74 (2017); https://doi.org/10.1016/j.cej.2016.08.067
20. J. Iqbal, B.A. Abbasi, R. Batool, A.T. Khalil, S. Hameed, S. Kanwal, I. Ullah and T. Mahmood, *Mater. Res. Express*, **6**, 115407 (2019); https://doi.org/10.1088/2053-1591/ab4f04
21. I. Hussain, N.B. Singh, A. Singh, H. Singh and S.C. Singh, *Biotechnol. Lett.*, **38**, 545 (2016); https://doi.org/10.1007/s10529-015-2026-7
22. V.T. Chagas, L.M. França, S. Malik and A.M.A. Paes, *Front. Pharmacol.*, **6**, 259 (2015); https://doi.org/10.3389/fphar.2015.00259
23. M. Ayyanar and P. Subash-Babu, *Asian Pac. J. Trop. Biomed.*, **2**, 240 (2012); https://doi.org/10.1016/S2221-1691(12)60050-1
24. A. Kumar, T. Jayachandran, P. Aravindhan, D. Deecaraman, R. Ilavarasan and N. Padmanadhan, *Afr. J. Pharm. Pharmacol.*, **3**, 560 (2009).
25. M.A. Asghar, E. Zahir, M.A. Asghar, J. Iqbal and A.A. Rehman, *PLoS One*, **15**, e0234964 (2020); https://doi.org/10.1371/journal.pone.0234964
26. V. Kumar, S.C. Yadav and S.K. Yadav, *J. Chem. Technol. Biotechnol.*, **85**, 1301 (2010); https://doi.org/10.1002/jctb.2427
27. S.H. Kumar, Ch. Prasad, S. Venkateswarlu, P. Venkateswarlu and N.V.V. Jyothi, *Adv. Chem. Sci.*, **3**, 299 (2015).
28. M. Rafique, R. Tahir, S.S.A. Gillani, M.B. Tahir, M. Shakil, T. Iqbal and M.O. Abdellahi, *Int. J. Environ. Anal. Chem.*, **102**, 23 (2022); https://doi.org/10.1080/03067319.2020.1715379
29. A. Kalam, A.G. Al-Sehemi, A.S. Al-Shihri, G. Du and T. Ahmad, *Mater. Charact.*, **68**, 77 (2012); https://doi.org/10.1016/j.matchar.2012.03.011
30. K. Kannan, D. Radhika, M.P. Nikolova, K.K. Sadasivuni, H. Mahdizadeh and U. Verma, *Inorg. Chem. Commun.*, **113**, 107755 (2020); https://doi.org/10.1016/j.inoche.2019.107755
31. A. Kumar and C.K. Dixit, Methods for Characterization of Nanoparticles, In: Advances in Nanomedicine for the Delivery of Therapeutic Nucleic Acids, Woodhead Publishing, pp. 43-58 (2017).
32. K.N. Yu, T.-J. Yoon, A. Minai-Tehrani, J.-E. Kim, S.J. Park, M.S. Jeong, S.-W. Ha, J.-K. Lee, J.S. Kim and M.-H. Cho, *Toxicol. In Vitro*, **27**, 1187 (2013); https://doi.org/10.1016/j.tiv.2013.02.010